

Rotational g factors of osmium isotopes at low spins

A. Ansari

*Institute of Physics, Bhubaneswar-751005, India
and International Centre for Theoretical Physics, Trieste, Italy*

(Received 4 December 1987)

In view of recent experimental data on g factors of osmium isotopes which show interesting variations as a function of mass number as well as spin, we have calculated these following the methods of variation after exact angular momentum projection of axial Hartree-Fock-Bogoliubov wave functions and the cranked Hartree-Fock-Bogoliubov theory. The observed trend of the variation of g factor at $I=2$ with the mass number $A=186-192$ is reproduced with very minor adjustments of the force constants of the employed pairing-plus-quadrupole model Hamiltonian in both the approaches. However, the variation of g factor with spin, which is sensitive to the interplay between collective and single particle degrees of freedom, can be understood only in the cranking approach. Though these nuclei are prolate in shape, with the increase of A they become more and more γ soft and we suggest that γ deformation should be treated in a generator coordinate type of calculation.

I. INTRODUCTION

From the sign of the static electric quadrupole moments of the first excited 2^+ states (Q_2^+) of osmium isotopes Kumar and Baranger^{1,2} predicted that the ground-state shapes of these nuclei are prolate for the mass numbers up to $A=192$. Cline³ also finds from the Coulomb excitation measurements of Q_2^+ that $A=186-192$ Os isotopes are prolate, not only in the ground state but even for low-spin excited states. Very recently Gaypong *et al.*⁴ have reported on Q_2^+ measurements of ¹⁹²Pt and have discussed that in Pt isotopes prolate to oblate shape transition takes place around $A=188$, whereas Os isotopes are prolate until $A=192$.

On the other hand, the studies of g factors of the excited states reveal fine structures of the nuclear wave functions and data on g factors would supplement the structure informations obtained from Q_2^+ measurements. In a recent lecture Benczer-Koller⁵ has presented a detailed account of the experimental measurements of g factors and their impact on the studies of the nuclear structure. Since the last few years the Melbourne group⁶⁻¹⁰ has been particularly active on g -factor measurements and has made a very critical analysis of the available theoretical models, particularly phenomenological interacting boson approximation (IBM-1) and proton-neutron interacting boson approximation (IBM-2) models,¹¹ in light of understanding simultaneously the behavior of g factors as a function of mass number as well as spin of the excited states of a nucleus. The interacting boson approximation (IBA) models need too many parameters, though Sambataro *et al.*¹¹ are able to produce the variation of g factor

at $I=2$ (i.e., g_2) with A for the osmium isotopes. It is an interesting observation^{7,8} that g_2 increase with the increase of A (Z/A decreases by 3% in going from ¹⁸⁶Os to ¹⁹²Os), whereas the ratio g_4/g_2 exhibits the opposite trend, i.e., decreases with the increase of A from $A=188$ to 192. The value $g_4 > g_2$ for ^{188,190}Os and $g_4 \approx g_2$ for ¹⁹²Os. In order to understand the dynamics or mechanism responsible for these variations we have applied cranked Hartree-Fock-Bogoliubov (CHFb) theory¹²⁻¹⁴ as well as the approach of variation after exact angular momentum projection from an axially symmetric HFB wave function (AXVAP).^{15,16} The potential energy surfaces¹⁷ of these nuclei being shallow in the β - γ space the cranking method is not very much justified. However, this is the simplest available microscopic approach to allow for the rotation alignment of the single particle (sp) orbitals in order to generate the angular momenta of the excited states. It may be interesting to see the response of cranking on the proton and neutron orbitals because it is the competition between these two which decides the resultant value of the g factor.

In Sec. II we outline the theoretical framework for calculations presenting the results and discussions in Sec. III. Then conclusions of the present investigations are briefly summarized in Sec. IV.

II. THEORETICAL FRAMEWORK

The ground-state properties of the nuclei considered here have been calculated in the standard HFB theory^{17,18} employing the pairing plus quadrupole model Hamiltonian of Baranger and Kumar^{1,18} (BK)

$$H = \sum_{\alpha, \tau} \epsilon_{\alpha} c_{\alpha}^{\dagger} c_{\alpha} - \frac{1}{2} \sum_{\lambda=2,4} \chi_{\lambda} \sum_{\alpha\beta\gamma\delta} \alpha_{\sigma} \alpha_{\tau} \langle \alpha | Q_{\lambda\mu}^{\sigma} | \gamma \rangle \langle \beta | (-1)^{\mu} Q_{\lambda-\mu}^{\tau} | \delta \rangle c_{\alpha}^{\dagger} c_{\beta}^{\dagger} c_{\delta} c_{\gamma} - \frac{1}{4} \sum_{\tau} G_{\tau} \sum_{\alpha\gamma} c_{\alpha}^{\dagger} c_{\alpha}^{\dagger} c_{\bar{\alpha}} c_{\bar{\gamma}} \quad (1)$$

Various symbols have their usual meaning σ, τ being proton or neutron and, in general,

$$Q_{\lambda\mu} = r^2 Y_{\lambda\mu}(\theta, \phi). \quad (2)$$

Recently¹⁷ we have studied the shape transition properties in the Os-Pt region using the above Hamiltonian with spherical single particle (sp) energies ϵ_α taken from Ref. 18. We shall refer to this as the BK-I Hamiltonian. We have repeated these calculations using sp energies from a later paper of BK (Ref. 1) which are readjusted values of the previous¹⁸ version. With these the inclusion of the hexadecapole, $\lambda=4$, term is not very essential, or we may say that its importance is reduced. Using the following sets of the force constants (all in MeV)

$$\chi_2 = 75/A^{1.4}, \quad G_p = 28/A, \quad G_n = 22/A, \quad (3)$$

we find¹⁹ that ^{186–192}Os come out to be prolate in the ground state, though ¹⁹²Os develops a good well-localized minimum at $\gamma=0$ only if the $\lambda=4$ term is also considered. Then treating these nuclei as prolate ones the behavior of g factors as a function of mass number ($A=186–192$) and spin (I) are investigated through the AXVAP (Refs. 13, 15, and 16) and CHFb (Refs 12–16) approaches. We have also studied the sensitivity of g factors on the values of various force constants.

$$\mu_I = \frac{I}{\sqrt{I(I+1)}} \frac{\int_0^{\pi/2} d\theta \sin\theta d_{-10}^I(\theta) \sum_{\tau} \langle \Psi_{\text{HFB}} | \hat{\mu}_{\tau} e^{-i\theta j_y} | \Psi_{\text{HFB}} \rangle}{\int_0^{\pi/2} d\theta \sin\theta d_{00}^I(\theta) N(\theta)}, \quad (6)$$

where $d(\theta)$ is the rotation matrix, θ being the angle of rotation about the Y axis. $N(\theta)$ is the overlap kernel

$$N(\theta) = \langle \Psi_{\text{HFB}} | e^{-i\theta j_y} | \Psi_{\text{HFB}} \rangle, \quad (7)$$

and, with the usual definition of step up operators, we have

$$\hat{\mu}_+ = g_l \sum_i \hat{I}_+(i) + g_s \sum_i \hat{s}_+(i), \quad (8)$$

where values of the free particle g factors are $g_l=1$, $g_s=5.586$ for protons and $g_l=0$ and $g_s=-3.826$ for neutrons. In numerical calculations we use the attenuated²² values of the spin g factors as $g_s=0.6g_s(\text{free})$. Then finally the g factor for a state I is calculated from

$$\mu_I = I g_I. \quad (9)$$

B. CHFb approach

This is also a well-known method^{12–15} where the Hamiltonian is cranked about an axis perpendicular to the symmetry axis (here X axis) of the nucleus

$$H^\omega = H - \omega \hat{J}_X, \quad (10)$$

where ω is a Lagrange multiplier or the rotational fre-

A. AXVAP approach

The method of angular momentum projection is well known,^{13,15,16} so we will not give any details here. The spin projected energy, $E_I(\beta, \Delta_p, \Delta_n)$ is minimized with respect to the axial quadrupole deformation parameter β and proton and neutron pairing gaps Δ_p and Δ_n , respectively. We should mention that instead of performing the particle number projection on the spin projected HFB wave function (Ψ_I), we only apply corrections^{16,20} to the energy E_I due to errors in the expectation values of the number operators compared to the correct numbers N_p^0 or N_n^0 :

$$E_I^C = E_I - \lambda_p \delta N_p - \lambda_n \delta N_n, \quad (4)$$

where

$$\delta N = \langle \Psi_I | \hat{N} | \Psi_I \rangle - N^0 \quad (5)$$

and λ_p, λ_n are the Fermi energies for protons and neutrons, respectively. It is this energy E_I^C which is minimized with respect to the shape parameters β , Δ_p , and Δ_n for a given I . These number corrections are rather important for the energy spectrum (for a good discussion on this see Ref. 16), but otherwise number projection does not affect^{14,16} significantly the values of g factors. Then corresponding to the minimum of the energy E_I^C the wave function is used to calculate the magnetic moment²¹

quency such that the total angular momentum of the system is given by the constraint

$$I_X = \langle \Psi_{\text{CHFb}}(\omega) | \hat{J}_X | \Psi_{\text{CHFb}}(\omega) \rangle = \sqrt{I(I+1)}, \quad (11)$$

along with the usual constraint on the particle number, N^0

$$\langle \Psi_{\text{CHFb}}(\omega) | \hat{N} | \Psi_{\text{CHFb}}(\omega) \rangle = N^0. \quad (12)$$

For any small numerical error in the relation (12) we correct the energy as in Eq. (4).

Finally, g factors are computed from the expectation values of the X component of magnetic moment operator^{14,23} as

$$g_I = \langle \Psi_{\text{CHFb}} | \hat{\mu}_X | \Psi_{\text{CHFb}} \rangle / I_X, \quad (13)$$

where

$$\hat{\mu}_X = g_l \sum_i \hat{j}_X(i) + (g_s - g_l) \sum_i \hat{s}_X(i), \quad (14)$$

with the single particle g values as mentioned earlier. Putting the numerical values of g_l and g_s (attenuated by a factor of 0.6) we can cast (13) in a useful transparent form

$$\sqrt{I(I+1)} g_I = I_X^l + 2.351 (\langle \hat{S}_X \rangle^p - 0.98 \langle \hat{S}_X \rangle^n). \quad (15)$$

TABLE I. Variation of g factor at $I=2$ with the mass number of osmium isotopes in the AXVAP approach. The experimental values are listed in the seventh column. The force constants $\chi_2=75/A^{1.4}$, $G_n=22/A$, and G_p are listed in the second column.

A	AG_p	β	Δ_p	Δ_n	g_2	g_2^{expt}	I^n/I
186	28	0.239	0.654	1.059	0.292	0.282 ± 0.007	0.704
188	28	0.215	0.663	1.063	0.309	0.292 ± 0.010	0.686
190	27	0.200	0.594	1.012	0.332	0.350 ± 0.011	0.664
192	27	0.183	0.598	0.941	0.335	0.396 ± 0.010	0.660

In the above the superscripts p or n denote proton or neutron contributions. The sign of the second term indicates the dominance of the relative alignment of proton or neutron orbitals. Of course, when there is a rotation alignment the orbital contribution affects significantly the value of I_X^p also. The contribution of the second term in (15) to the total g_I will be denoted (for convenience in later discussions) by g_{SAL} (spin aligned contribution). It may be noted that without cranking when the time reversal symmetry is respected $\langle S_X \rangle = 0$.

III. RESULTS AND DISCUSSIONS

A. g factors in AXVAP approach

As far as the variation of g factor of the first excited 2^+ state (g_2) with A is concerned, it should mainly depend on how realistic is the choice of the Hamiltonian of the system. As will be seen, because of a smooth A dependence of the sp energies as well as other force constants, we do have some difficulty in reproducing g_2 vs A behavior towards ^{192}Os . Using Eqs. (6) and (9) for $I=2, 4$, and 6 we have calculated g factors of $^{186-192}\text{Os}$. For a given nucleus the g factors remain almost a constant for the low spins considered here. For instance, in case of ^{188}Os we get $g_I=0.308, 0.302$, and 0.298 for $I=2, 4$, and 6 , respectively. Thus, the observed trend of $g_4 > g_2$ is not coming out in the AXVAP approach. On the other hand, for $I=2$ we get a very satisfactory result, as enumerated in Table I. To get a correct trend of increasing g_2 value with the increase of A we need to reduce a little proton pairing for $^{190,192}\text{Os}$, and we have taken $G_p=27/A$. With a further decrease of G_p by less than 1% for ^{192}Os the agreement can be very much improved. In Sec. III B we shall discuss more about the effect of various force constants on g factors. It is a surprising coincidence that the magnitudes of the calculated numbers are very close to the experimental values.⁶⁻⁸ The last column of Table I shows the fractional angular momentum contribution of neutrons to the total spin ($I=2$) for various isotopes. We notice that this ratio goes decreasing with the increase of A , i.e., N . This is essential to get the correct trend of g_2 values with A .

The variation of g factor with I is better understood in the cranking approach which we discuss next.

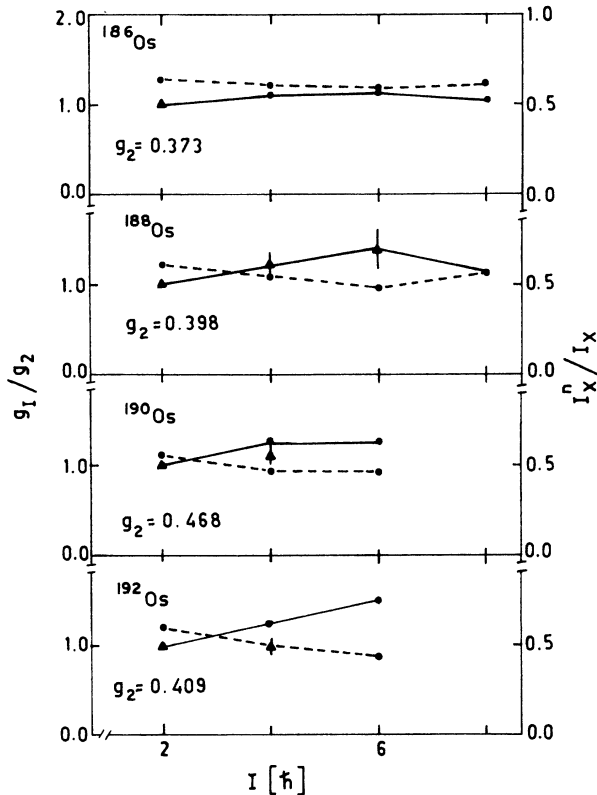


FIG. 1. Variation of g_I/g_2 as a function of spin I for $^{186-192}\text{Os}$ shown by solid lines. The numerical value of the g factor at $I=2$ for each isotope is written on the figure. The solid triangles (\blacktriangle) with the error bars denote the experimental values. Variation of the ratio I_X^n/I_X with total spin is indicated by the dashed curves for which the scale is marked on the right-hand side.

TABLE II. Ratio of proton-to-neutron contributions to the total angular momentum as well as to the expectation value of the spin operator and their variations with the mass number. $\chi_2=75/A^{1.4}$, $G_p=28/A$, and $G_n=22/A$. The numbers in the brackets correspond to $G_p=27/A$.

A	I_X^p/I_X^n	S_X^p/S_X^n	$g_R = I_X^p/I_X^n$
186	0.587	1.038	0.370
188	0.652	1.053	0.395
190	0.634	0.907	0.388
	(0.826)	(1.300)	(0.452)
192	0.528	0.711	0.346
	(0.710)	(1.015)	(0.407)

B. g factors in the CHFb approach

After the solution of the cranked HFB equations^{12–14} with the particle number and angular momentum constraints, Eqs. (11) and (12), we calculate g factors using the relation (15). In Fig. 1 we have displayed the variation of g_I/g_2 as a function of spin for $A = 186–192$. The force constants are the same as used in the AXVAP scheme (Table I). Theoretical value of g_2 for each isotope is written on the figure and we find that due to a little too much alignment of proton $h_{11/2}$ ($m = \frac{7}{2}, \frac{9}{2}$) orbitals these are larger than the experimental values, which are listed in Table I. But the correct trend of the variation of g_2 with A can be reproduced with small adjustments of G_p for ^{190,192}Os. For example, with $G_p = 26.75/A$ for ¹⁹²Os we get $g_2 = 0.442$ compared to 0.409 when $G_p = 27/A$. The available experimental data^{6–8} are shown by solid triangles and, particularly for ¹⁸⁸Os computed numbers, agree quite well. For ¹⁹²Os we find g_I increasing with I as in the case of lighter isotopes. But we must point out¹⁹ that with the present pairing plus quadrupole Hamiltonian ¹⁹²Os does not come out to be a good prolate deformed nucleus. The energy surface remains very flat in the γ direction. With increasing spin the alignment of proton orbitals need to be counterbalanced by $i_{13/2}$ neutron alignments. However, it is not clear how to achieve this except that in the AXVAP calculation we get almost a constant value for g_I .

In Fig. 1 we have also shown, by dashed curves, the variation of fractional contribution of neutrons to the total spin, I_n^x/I_x , as a function of I for each isotope. For this the scale is marked on the right-hand side. Due to a partial rotation alignment of $h_{11/2}$ protons this is decreasing up to $I = 6$. Then at $I = 8$ for ^{186,188}Os I_n^x/I_x exhibits an increase due to the alignment of $i_{13/2}$ neutrons. Thus we expect that for $I \geq 8$ for ^{186,188}Os, g factors will decrease with I . We should mention that we have done these calculations only for one spin beyond a state for which the experimental data are available.

Next we have looked for some systematics as to how changes in the values of various force constants of the Hamiltonian affect the behavior of g factors. These can be seen through Tables II–V. The ratio of proton-to-neutron contributions to the total angular momentum at $I = 2$ for various isotopes is listed in Table II. The variation of g_2 with A is essentially related to the variation of this ratio. We know that $\langle \Psi_{\text{CHFb}} | \hat{S}_X | \Psi_{\text{CHFb}} \rangle = 0$ in the ground state as the time reversal symmetry is strictly respected. However, in a cranking calculation for $I > 0$ its value depends on the degree of rotation alignment (of course, time reversal symmetry is broken). So we have also listed in the second column S_X^p/S_X^n to show that the behavior of this quantity is also directly related to the behavior of g factors as a function of A . In fact, the same is true even for the trend of the variation of g factors as a function of spin. The last column gives the pure rotational values of g factors to which addition of g_{SAL} , the contribution of the second term of Eq. (15), would give the total g factor. The numbers in the brackets for ^{190,192}Os correspond to a weaker proton pairing ($G_p = 27/A$) which allows for a larger proton alignment.

In Tables III–V we have attempted to demonstrate the dependence or sensitivity of g factors on various force constants of the Hamiltonian. It would give an idea of the relative importance of various factors responsible to control the behavior of g factors as a function of mass number as well as spin. It may provide some guide lines for the phenomenological studies of these properties as in IBA models.¹¹ Table III shows that for ¹⁸⁸Os g_2 changes only by about 2% if χ_2 changes by about 10%. That is, change in the collective quadrupole variables does not much affect the value of the g factor at $I = 2$. On the other hand, at higher spins it could be important, which we demonstrate in Table IV. Changes in χ_2 (or deformation β) can affect the alignment considerably which is reflected from the values of g_{SAL} as a function of I . Here we notice that with smaller χ_2 neutron alignment dominates.

Results of Table V exhibit the sensitivity of g factor at $I = 2$ to the values of G_p with fixed values of χ_2 and G_n for ^{186,188}Os. Since there is not much alignment at $I = 2$ we find a direct relation between the change in Δ_p (caused by change in G_p) and the change in the value of g_2 . In the last row experimental values are listed which could be almost exactly reproduced by adjusting G_p (or maybe even G_n , which we have not tried). These results show that values of g factors are more sensitive to the changes in pair correlations as a small change in pairing can easily modify the single particle occupation probabilities near the Fermi surface.

C. g factors of ¹⁸⁸Os using BK-I Hamiltonian plus a hexadecapole term (Ref. 17)

Out of the four osmium isotopes considered here, maximum information on g factors is available for ¹⁸⁸Os, and according to our previous¹⁷ calculation it is a good prolate nucleus. So, taking the BK-I Hamiltonian with the force constants as¹⁷

$$\chi_2 = \chi_4 = 70/A^{1.4}, \quad G_p = 28/A, \quad G_n = 23/A. \quad (16)$$

We have computed g factors and other intrinsic shape parameters as listed in Table VI for $I = 0–12$. We may mention *a priori* that with less pairing and stronger hexadecapole force the nucleus remains prolate till higher spins, and this seems to be favored by the experimental information.^{3,4} The available experimental values of g factors are listed in the last column of the Table VI. Instead of any increase we get $g_4 \approx g_2$. The rotational frequencies ω show backbending features at $I = 10–12$ due mainly to $i_{13/2}$ neutron alignment. Experimentally²⁴ this is expected at $I \sim 14$. Also associated with the alignment a strong γ asymmetry develops at $I = 10–12$.

As we have learned from the preceding sections that g factors are very sensitive to changes in pairing, we have tried to allow for a little more alignment of protons (e.g., see the column under g_{SAL}) by decreasing G_p [Eq. (16)] to the value $G_p = 27/A$. With this small change all the calculated quantities presented in the Table VI are listed again in Table VII in order to have a clear comparison. As a function of spin, most notable differences are in the values of ω , γ , Δ_p , and consequently g_I . The backbending point has shifted to a higher spin value, and g_4 has in-

TABLE III. Effect of variation of χ_2 on g factor at $I=2$ for ^{188}Os . $G_p=28/A$, and $G_n=22/A$. The values of γ are in degrees.

χ_2	g_2	g_2^{expt}	β	γ	Δ_p	Δ_n
78	0.401	0.292 ± 0.010	0.231	7.1	0.519	0.909
75	0.398		0.208	4.6	0.560	0.921
72	0.396		0.187	3.1	0.591	0.939
70	0.392		0.180	3.6	0.602	0.943

TABLE IV. Effect of variation of χ_2 on g_{SAL} , i.e., the relative alignments of protons and neutrons at $I=2, 4, 6$ in ^{188}Os . $G_p=28/A$ and $G_n=22/A$. Headings 70, 72, 75, and 78 are values of χ_2 .

I	70		72		75		78	
	g	g_{SAL}	g	g_{SAL}	g	g_{SAL}	g	g_{SAL}
2	0.392	-0.001	0.396	0.000	0.398	0.004	0.401	0.008
4	0.319	-0.024	0.428	0.007	0.479	0.022	0.440	0.018
6	0.139	-0.075	0.341	-0.019	0.560	0.043	0.497	0.032

TABLE V. Effect of variation of G_p on g_2 of ^{186}Os and ^{188}Os . $\chi_2=70/A^{1.4}$ and $G_n=22/A$.

AG_p	Δ_p	^{186}Os		^{188}Os		
		I_X^p/I_X^n	g_2	Δ_p	I_X^p/I_X^n	g_2
28	0.598	0.591	0.369	0.602	0.646	0.392
29	0.704	0.464	0.299	0.676	0.532	0.335
29.2				0.751	0.458	0.291
29.4	0.746	0.435	0.280	0.771	0.437	0.278
Expt.			0.282 ± 0.007			0.292 ± 0.010

TABLE VI. Self-consistent CHFB results for ^{188}Os along with g factors. Hamiltonian used is BK-I plus hexadecapole as in Ref. 17. The values of γ are in degrees.

I	ω	β	γ	β_4	Δ_p	Δ_n	g_I	g_{SAL}	g^{expt}
0	0.0	0.204	0.0	-0.056	0.728	0.969			
2	0.1582	0.206	1.1	-0.058	0.695	0.936	0.364	0.011	0.292 ± 0.010
4	0.2415	0.209	3.9	-0.059	0.632	0.883	0.366	0.010	0.385 ± 0.035
6	0.2879	0.211	6.0	-0.060	0.559	0.821	0.352	0.004	0.412 ± 0.063
8	0.3098	0.211	9.4	-0.058	0.500	0.774	0.326	-0.006	
10	0.2996	0.209	17.2	-0.051	0.478	0.755	0.277	-0.025	
12	0.2584	0.204	27.7	-0.040	0.600	0.745	0.127	-0.075	

TABLE VII. Similar to Table VI with $G_p=27/A$. The values of γ are in degrees.

I	ω	β	γ	β_4	Δ_p	Δ_n	g_I	g_{SAL}
0	0.0	0.205	0.0	-0.058	0.614	0.962		
2	0.1477	0.208	1.2	-0.059	0.572	0.932	0.410	0.020
4	0.2287	0.210	3.9	-0.061	0.493	0.887	0.423	0.022
6	0.2781	0.211	5.9	-0.061	0.396	0.831	0.418	0.019
8	0.3062	0.212	7.1	-0.061	0.289	0.776	0.393	0.012
10	0.3192	0.211	10.0	-0.058	0.212	0.729	0.355	-0.001
12	0.2923	0.209	20.0	-0.049	0.146	0.727	0.323	-0.017

creased compared to g_2 by about 3%. Even the γ energies, $E_\gamma(I) = E_I - E_{I-2}$, come out quite reasonable being (in keV) 192, 389, 511, 566, 622, and 577 compared to the experimental²⁴ numbers of 155, 323, 462, 575, 655, and 686, respectively, for $I = 2-12$.

IV. CONCLUSIONS

From these parameter-free microscopic calculations we find that the increasing trend of g_2 with the increase of A for $^{186,188}\text{Os}$ clearly comes out. But for the heavier isotopes we have to make some small adjustments in the values of the force constants (χ or G). The variation of g_I/g_2 with I is well reproduced for ^{188}Os in the CHFB theory, the initial increase of the g factor being caused by a partial alignment of $h_{11/2}$ proton orbitals. This is followed by an alignment of $i_{13/2}$ neutrons at $I \simeq 8$, and we predict a decrease of g factors at higher spins. On the other hand, an almost constant experimental value of g_I

in $^{190,192}\text{Os}$ can be reproduced in the AXVAP approach but not in the cranking theory. However, for these heavier isotopes the potential energy surfaces are flat^{17,19} in the γ direction. Therefore, only after properly including the γ degrees of freedom in the description of the structure of these nuclei can one be sure of a correct theoretical understanding of their properties. Within the cranking approach we are planning to perform a generator coordinate type of calculation in the space of γ deformation parameter for $^{188-192}\text{Os}$ isotopes.

ACKNOWLEDGMENT

The author expresses his gratitude for the excellent facilities and hospitality at the International Centre for Theoretical Physics (ICTP) during a short visit as an Associate Member of the Centre when a part of the work was carried out. This work was also supported in part by the Department of Atomic Energy (DAE), Government of India.

¹K. Kumar and M. Baranger, Nucl. Phys. **A122**, 273 (1968).

²K. Kumar, Phys. Lett. **29B**, 25 (1969).

³D. Cline, Ann. Rev. Nucl. Part. Sci. **36**, 683 (1986).

⁴G. J. Gyapong, R. H. Spear, M. P. Fewell, A. M. Baxter, and S. M. Burnett., Nucl. Phys. **A470**, 415 (1987).

⁵N. Benczer-Koller, *Proceedings of the IX Workshop in Nuclear Physics*, Buenos Aires, 1986, edited by A. O. Macchiavelli, H. M. Sofia, and E. Ventura (World-Scientific, Singapore, 1986), p. 261.

⁶H. H. Bolotin, I. Morrison, C. G. Ryan, and A. E. Stuchbery, Nucl. Phys. **A401**, 175 (1983).

⁷A. E. Stuchbery, I. Morrison, and H. H. Bolotin, Phys. Lett. **139B**, 259 (1984).

⁸A. E. Stuchbery, I. Morrison, L. D. Wood, R. A. Bark, H. Yamada, and H. H. Bolotin, Nucl. Phys. **A435**, 635 (1985).

⁹A. E. Stuchbery, H. H. Bolotin, C. E. Doran, and A. P. Byrne, Z. Phys. A **322**, 287 (1985).

¹⁰A. P. Byrne, A. E. Stuchbery, H. H. Bolotin, C. E. Doran, and G. J. Lampard, Nucl. Phys. **A466**, 419 (1987).

¹¹M. Sambataro, O. Scholten, A. E. L. Dieperink, and G. Piccit-

to, Nucl. Phys. **A423**, 333 (1984).

¹²A. L. Goodman, Adv. Nucl. Phys. **11**, 263 (1979).

¹³P. Ring and P. Schuck, *The Nuclear Manybody Problems*, (Springer-Verlag, New York, 1980).

¹⁴A. Ansari, E. Wüst, and K. Muhlans, Nucl. Phys. **A415**, 215 (1985).

¹⁵A. Ansari and S. C. K. Nair, Nucl. Phys. **A283**, 326 (1977).

¹⁶E. Wüst, A. Ansari, and U. Mosel, Nucl. Phys. **A435**, 477 (1985).

¹⁷A. Ansari, Phys. Rev. C **33**, 321 (1986).

¹⁸M. Baranger and K. Kumar, Nucl. Phys. **A110**, 529 (1968).

¹⁹A. Ansari (unpublished).

²⁰K. Allart, K. Goeke, and A. Faessler, Z. Phys. A **263**, 407 (1973).

²¹A. Ansari and S. C. K. Nair, Phys. Rev. C (in press).

²²D. Schwalm, Nucl. Phys. **A396**, 339 (1983).

²³A. Ansari and S. C. K. Nair, Phys. Rev. C **25**, 1664 (1982).

²⁴R. A. Warner, I. M. Bernthal, J. S. Boyno, T. L. Khoo, and G. Sletten, Phys. Rev. Lett. **31**, 835 (1973).